RADIO AND X-RAY PROPERTIES OF MAGELLANIC CLOUD SUPERNOVA REMNANTS

J. R. Dickel
Astronomy Department, University of Illinois at Urbana-Champaign
1002 West Green Street, Urbana IL 61801, U.S.A.
JOHND@ASTRO.UIUC.EDU

Abstract

The Magellanic Clouds provides an invaluable sample of supernova remnants (SNRs) for comparative radio and X-ray morphological studies. The clouds contain a variety of remnants, all at the same distance. There are shell SNRs with thermal X-rays and non-thermal radio emission, pulsar wind nebulae (with and without observable pulsars) producing non-thermal radio and X-ray synchrotron emission, and composite objects containing both of these components. There are also mixed-morphology SNRs with shell radio emission and internal thermal X-rays. Often the X-ray and radio emission match well but sometimes they are surprisingly different in structure for reasons that are still being investigated.

1 Introduction

Approximately 50 supernova remnants (SNRs) in the Magellanic Clouds have been studied at both radio and X-ray wavelengths. As such they provide a good sample of remnants all at the same distance for comparative studies. We shall use examples from this population to illustrate the different types of SNRs and some of the information we can learn about them from the comparison of the emission in both wavelength regimes. Then we shall show some problem objects that we do not yet fully understand. Hopefully the next generation of telescopes will allow us to answer some of the questions posed by these SNRs.

2 Kinds of SNRs and their emission

2.1 Shell SNRs

Supernova remnants exhibit a variety of emission processes depending upon the location in the SNR and its type but almost all SNRs show a shell structure caused by the ejecta from the SN plowing up surrounding material. The SNR expansion is supersonic so there is a leading shock wave and also, in young remnants, a reverse shock going into the ejecta from the interface of the ejecta and the swept-up material. These shocks (also turbulence amplified at the interface) can accelerate particles to relativistic speeds to create synchrotron radiation. The swept-up shell accumulates mass and gradually slows as it expands. The de-acceleration initially depends upon the relative structure and mass of the expanding atmosphere and of the surroundings (Chevalier, 1982). After about eight times the ejected mass has been swept up, the ejecta become dynamically insignificant and the shell expands as if it were triggered by a point-blast (e.g., Sedov, 1959).

The synchrotron emission has a power-law spectrum with brighter intensity at longer wavelengths and often a short-wavelength, high-energy cutoff. The turbulence and Rayleigh-Taylor instabilities at the interface also amplify the ambient magnetic fields to enhance the synchrotron radiation and, in the younger remnants, create a radial pattern in the magnetic field structure. Figure 1 shows the radio emission from a young Type Ia SNR, N103B (Dickel & Milne, 1995).

Shells produce bright thermal X-rays from shock heated gas at temperatures of order 10^7 K or about 1 keV of energy. Spectral lines of highly ionized atoms are also visible in the X-ray spectra. Figure 2 shows the X-ray spectra of N103B and two other young SNRs in the LMC (Hughes et al., 1995).

As high energy X-ray detectors have improved we are finding that a number of SNRs show non-thermal X-ray emission from the region of the forward shock as first suggested for AD1006 by Becker et al. (1980). This implies a very strong magnetic field and other yet-to-be-explained acceleration processes (see, e.g.,

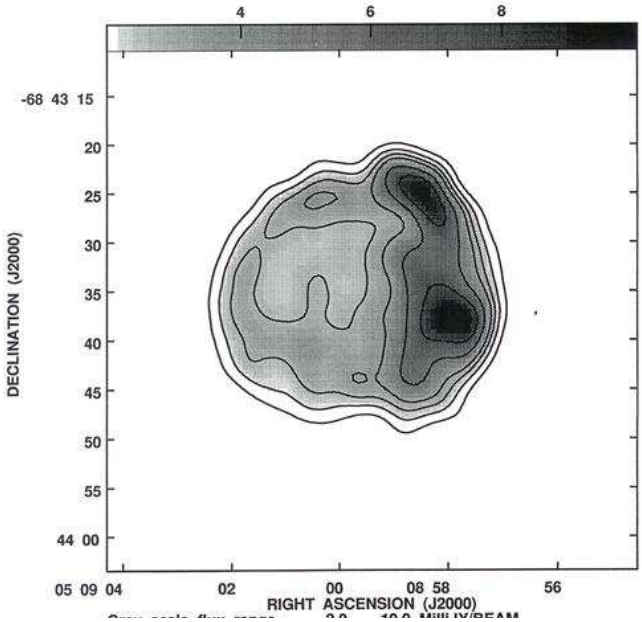

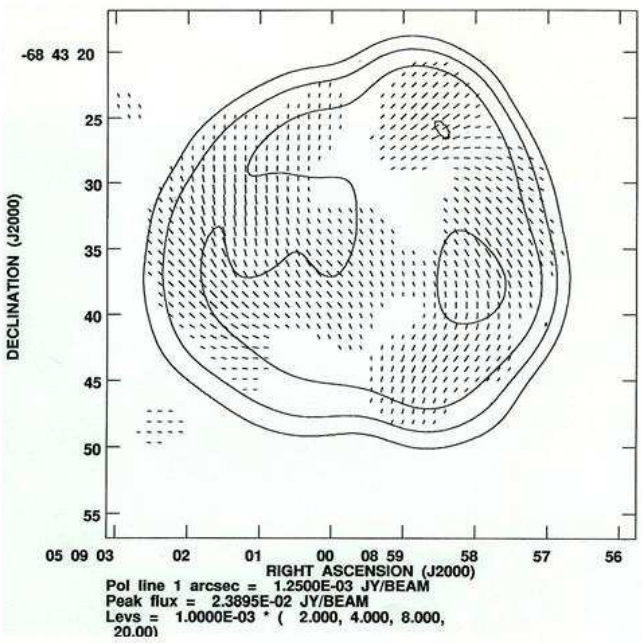

Figure 1: N103, a young SNR in the LMC. An H II region to the west is probably responsible for the asymmetry. The magnetic field vectors are approximately perpendicular to the ones shown suggesting a dominantly radial field.

Reynolds, 2005). While no synchrotron dominant SNR has been found in the Magellanic Clouds, this result is probably a selection effect based on sensitivity because of the large distances of 50 kpc to the LMC and 55 kpc to the SMC.

In older shell SNRs, dense, cool clumps will compress to retain pressure equilibrium with the hotter shocked

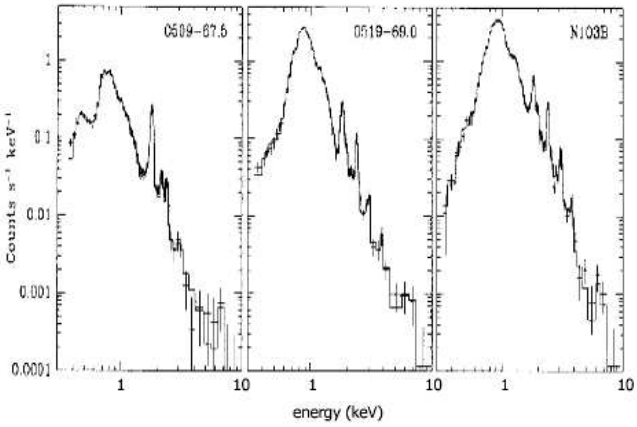

Figure 2: X-ray spectra of three young LMC SNRs including N103B on the right. They show the characteristic L-shell iron emission along with lines of several metals that are characteristic of Type Ia SNRs.

gas. The enhanced particle density and magnetic field strength increase the radio synchrotron emission so that we see a very tight correlation of optical and radio filaments. The bright X-rays often fill in the regions around the filaments.

The position angle of the polarized synchrotron emission appears to be rotated by Faraday rotation in the intervening ionized medium. The rotation is proportional to frequency^2 and so the rotation measure and the intrinsic magnetic field directions can be found by measurements at two frequencies. An example of this for N23 is shown in Fig. 3 (Dickel & Milne, 1998). The field appears to have tangential structure in some locations and mixed orientation in other places, not the predominantly radial structure found in the young, double-shock SNRs.

The rotation measure is proportional to $N_e \times \mathbf{B}$ and the X-ray emission is proportional to N_e^2. Therefore, if an SNR and its surroundings are sufficiently uniform, we can find a correlation between the square root of the X-ray emission and the Faraday rotation measure, as seen for N23 in Fig. 4. We can use the X-ray flux to determine the electron density and then use that in the rotation measure formula to evaluate the magnetic field strength along the line of sight. With some approximations for projections, we determine a magnetic field strength of 15 μGauss in N23. This is approximately 1/4 the relativistic particle energy or close to equipartition.

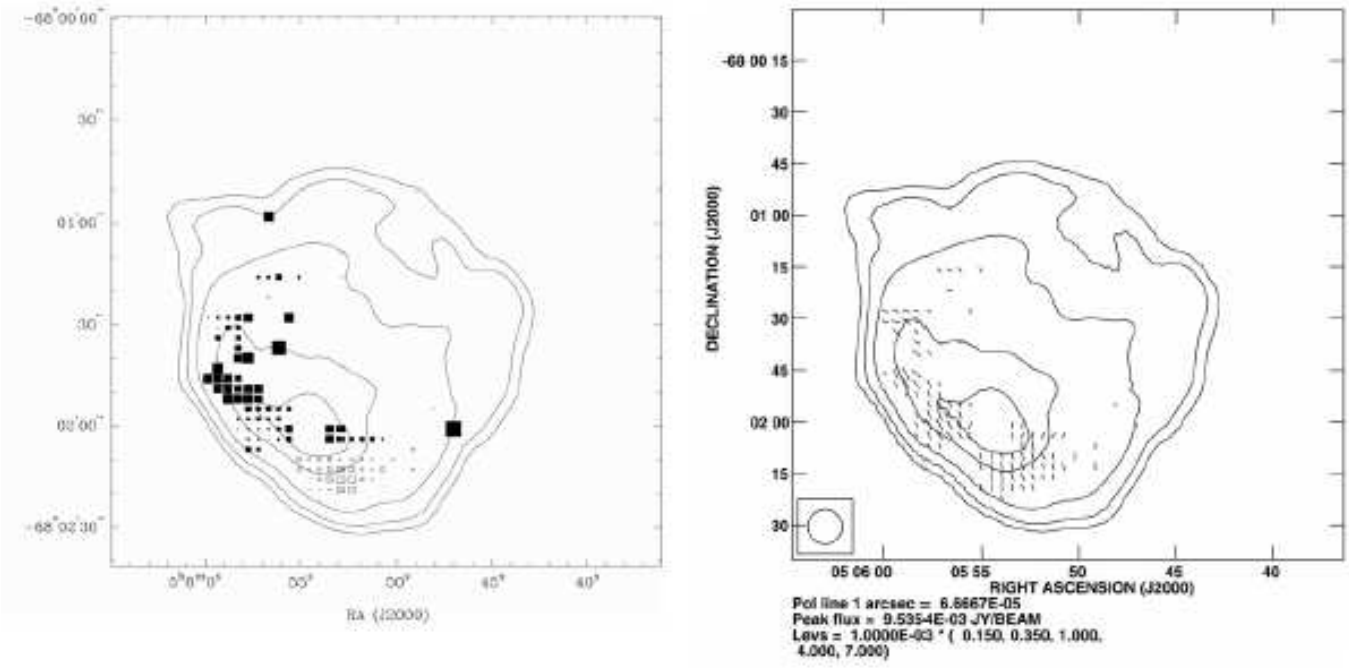

Figure 3: Faraday rotation and magnetic field vectors in the mature SNR N23.

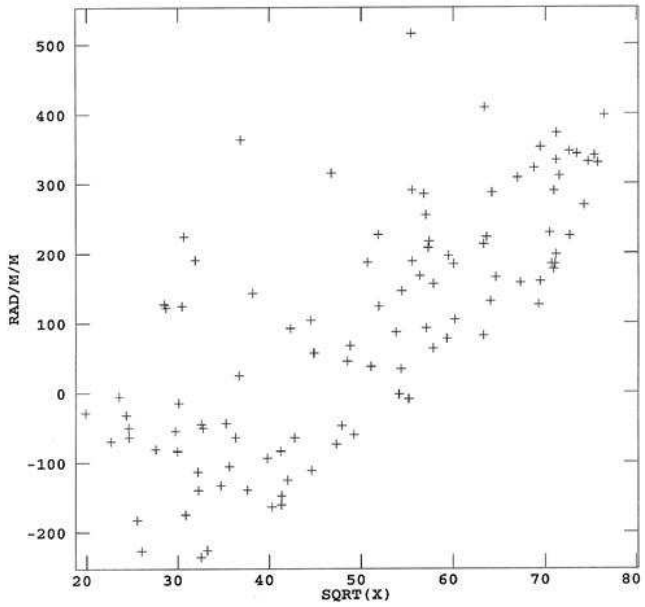

Figure 4: Correlation of the Faraday rotation with the square root of the X-ray intensity toward N23.

2.2 Pulsar wind nebulae and composite SNRs

Pulsars inject energetic particles into their environs which produce strong synchrotron radiation at radio through X-ray wavelengths. The synchrotron spectrum is flatter than that of typical shells but usually shows a break between the radio and X-ray regimes (the X-ray spectra is steeper). These pulsar wind nebulae (PWNs) are filled throughout and generally show very uniform magnetic fields. A good example of this type of remnant in the LMC is 0540−693. It also has a normal surrounding shell of synchrotron radio emission and thermal X-rays, making it a "composite" remnant. Figure 5 and 6 show the PWN and the entire SNR (Gotthelf & Wang, 2000; Dickel et al., 2002).

2.3 Mixed morphology SNRs

There are a few SNRs that show normal shell radio sources but reasonably smooth interior thermal X-rays. These are called "mixed morphology" remnants (Rho & Petre, 1998). They are likely to be caused by a combination of thermal conduction from the shock front into the interior (Cox et al., 1999; Shelton et al., 1999) and evaporation of clumps in the hot, low-density interior (White & Long, 1991). The only example of that class of SNR yet found in the LMC is the SNR part of N206 which also contains an apparent off-center pulsar wind nebula making it both a composite and a mixed morphology remnant (Williams et al., 2004).

3 Some interesting problems from comparisons of radio and X-ray images

Figure 7 shows a multi-wavelength comparison of the oxygen rich SNR 0102.2−7219 (Gaetz et al., 2000).

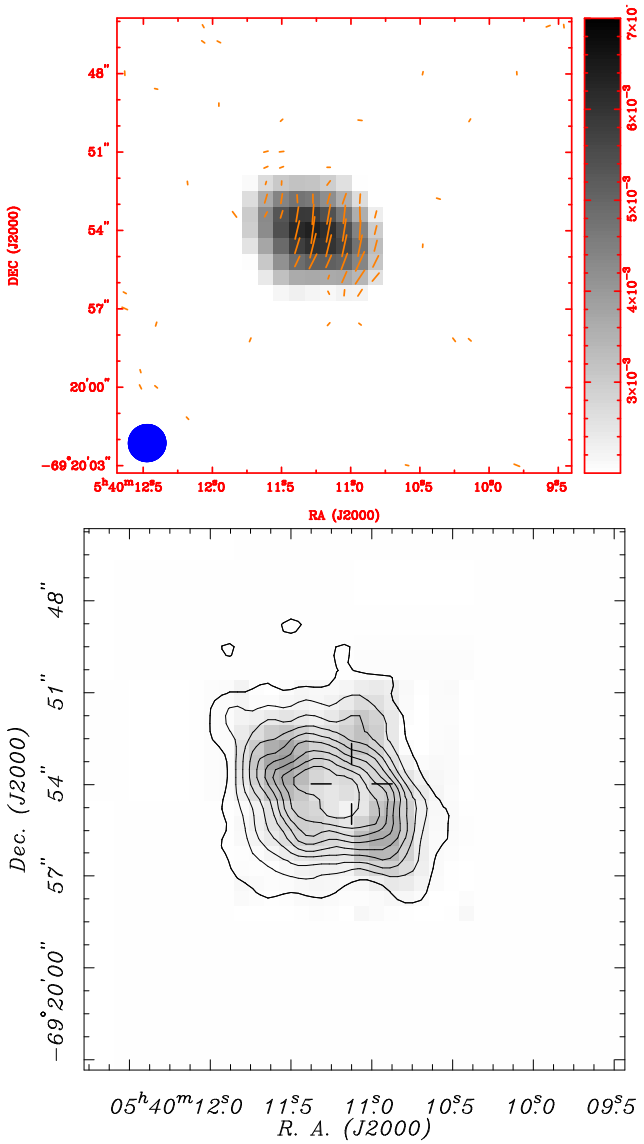

Figure 5: The PWN surrounding the 50-ms pulsar 0540−693 located at the center of the cross on the fight-hand image. Top: 6-cm radio image with magnetic field vectors. Bottom: X-ray contours and a higher resolution 3.5-cm radio grayscale.

Note that the radio emission sits outside the thermal shell X-ray emission, something not seen in other SNRs. Theory suggests that the X-rays should come from the gas heated by the outer shock and that much of the radio emission should be created inside by the reverse shock and turbulence at the interface of the ejecta and the swept-up material. A full explanation of this inversion is still needed.

SNR 0101−7226, also in the SMC, shows a normal radio shell but no X-ray emission. The few contours on the northwest edge are from an unrelated Be star (Hughes & Smith, 1994). The upper limit to the SNR X-ray emission in the 0.2–2.4 keV energy band is 9×10^{34} erg s^{-1} (Ye et al., 1995), over one hundred times fainter than typical SNRs whereas the radio surface brightness places it near the average for all remnants in Green's (2004) catalog of Galactic SNRs. The lack of coincidence between radio and X-ray candidate SNRs is quite typical in other galaxies. For example, Pannuti and colleagues (e.g., Pannuti et al., 2002, and references therein) have examined several galaxies in the local group and beyond and usually find an overlap of less than 20% between radio and X-ray SNR candidates. Although they suggest selection effects may explain some of the discrepancy, it is difficult to understand why remnants with with extremely bright radio luminosities go undetected in X-rays. We may still be missing some key factor in all comparisons of X-ray and radio brightnesses.

Another unusual SNR is N11L in the LMC. The images in Fig. 9 and the spectra in Fig. 10 show a one-sided "jet" structure and thermal radio emission from the extended region off the end of the jet (Williams et al., 1999). Could this be the remains of the ejection from a γ-ray burst when the SNR exploded? It is clear that better resolution and sensitivity are needed to fully separate the different components of this complex source.

One SNR in the LMC, N49, has within its boundary the site of the γ-ray event that occurred on March 5, 1979. It has since been found to fluctuate and is classified as the Soft Gamma-ray Repeater, SGR 0525−66[1] An X-ray point source coincides with the position of SGR 0525−66 but that position lies on the inner edge of the radio shell with no indication of enhanced radio or optical emission (Rothschild, Kulkarni & Lingenfelter, 1994; Dickel et al., 1995). It has been suggested that the object could be an anomalous X-ray pulsar but no X-ray pulses have been found (Kulkarni et al., 2003). The association of the various features needs further investigation.

4 The future

We certainly need greater sensitivity and resolution at both radio (the Square Kilometer Array) and X-ray (Constellation X) wavelengths as well as the contin-

[1]The name of that source is sometimes rounded up rather than truncated or shifted to J2000 without the J in the designation so it may be called SGR 0526−66 by some authors

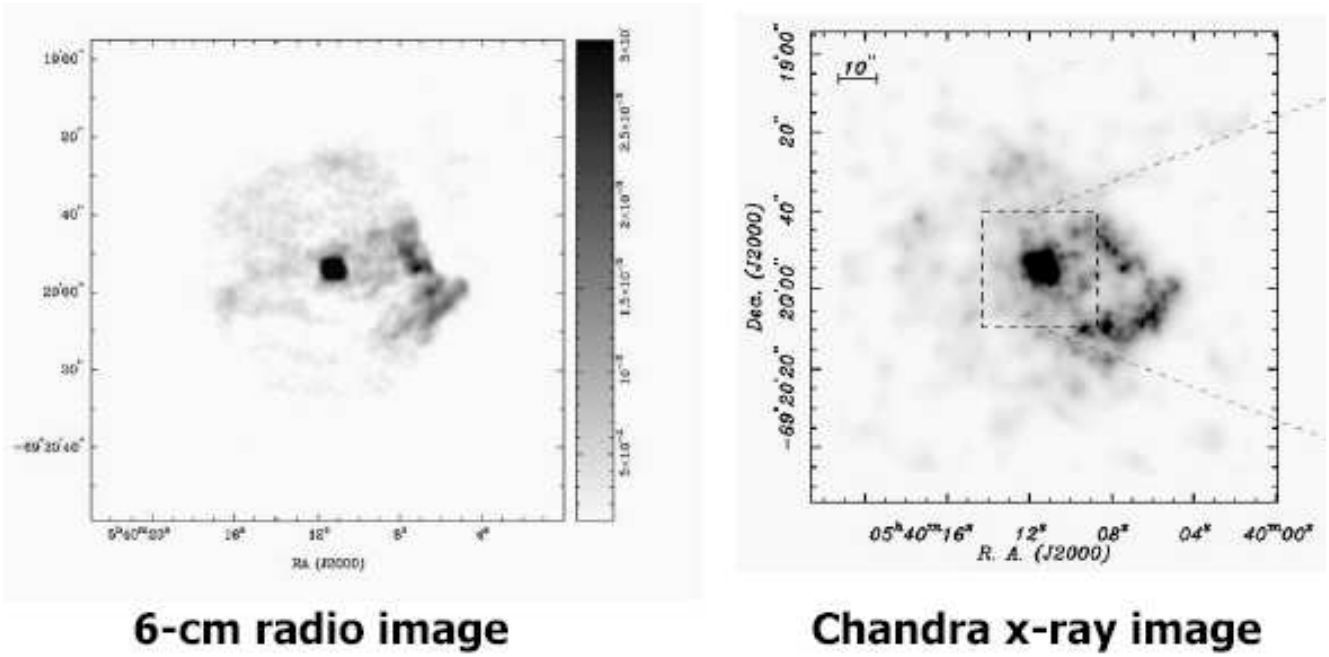

Figure 6: Radio and X-ray images of the entire composite SNR 0540−693. The radio emission is entirely non-thermal synchrotron radiation; the X-ray emission from the shell is thermal while that from the central PWN has the characteristic power-law spectrum of synchrotron radiation. The irregular shell is caused by the complex environment only 250 parsecs from the center of the huge 30 Doradus complex.

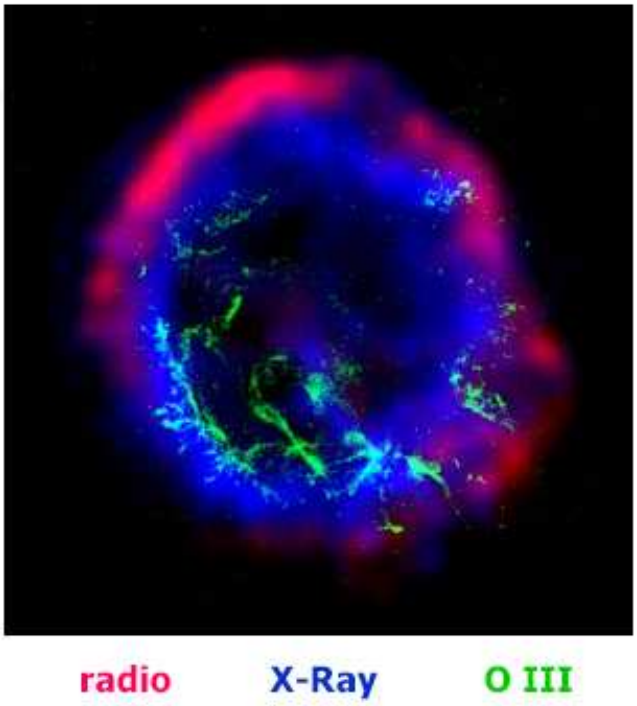

Figure 7: The SNR 0102−7219 in the SMC. The oxygen emission is in the forbidden line [O III] at 500.7 nm.

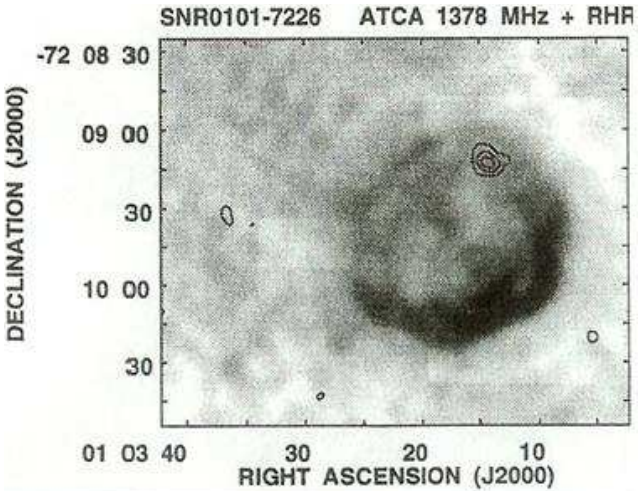

Figure 8: Radio grayscale and X-ray contours of the SNR 0101−7226.

ued growth of computer power according to Moore's law. Those results can help us to:

- Separate H II regions and SNR candidates in complex regions.
- Get X-ray spectra of individual clumps to see the detailed interactions of the expanding shells with the surroundings. They can then be bet-

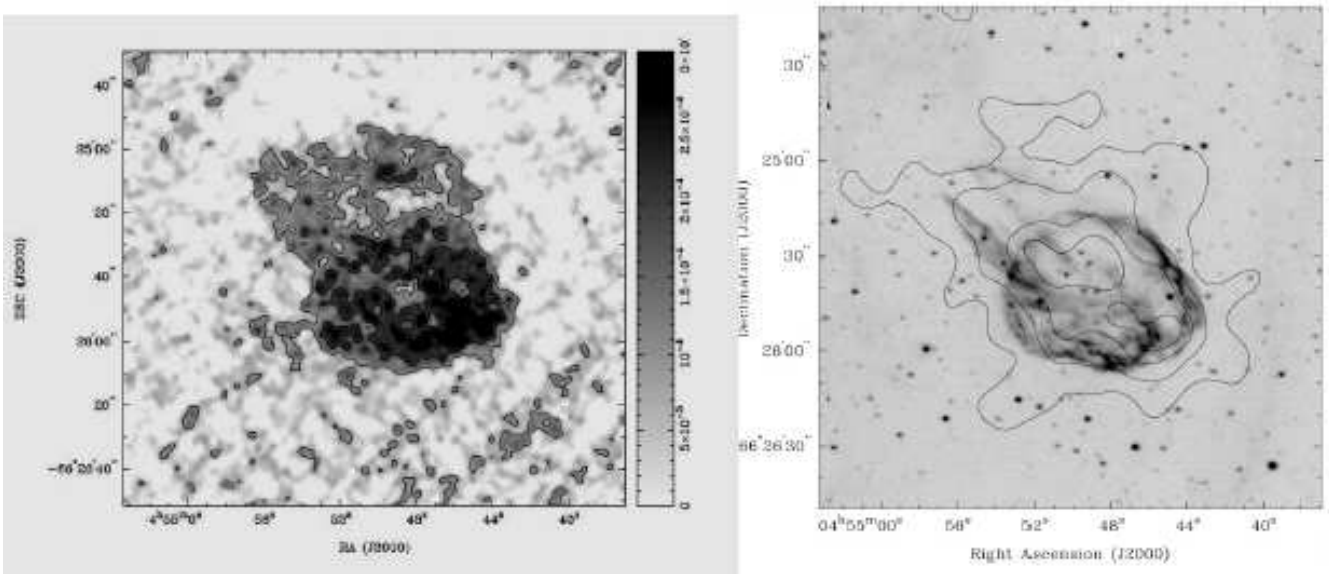

Figure 9: Left: 6-cm radio emission from N11L. Right: X-ray contours on an Hα image. The unusual "jet" and tail emerging from this shell SNR is visible somewhat differently in all three wavelength regimes.

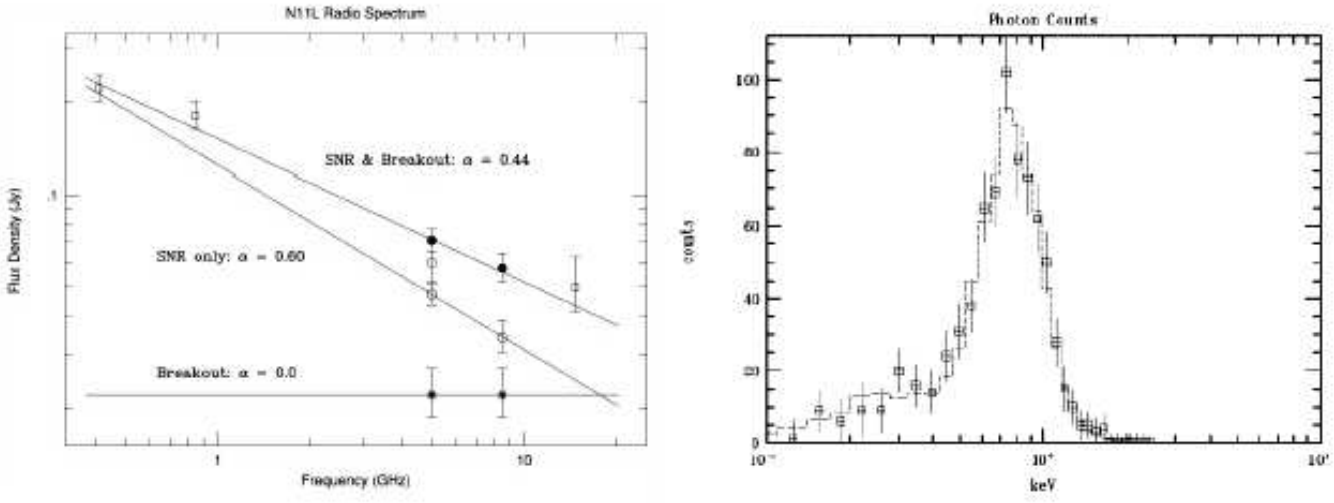

Figure 10: Radio (left) and X-ray (right) spectra of N11L. The breakout region has a flat radio spectrum and could be thermal whereas the steeper spectrum of the SNR is that of synchrotron emission from a relatively young remnant. The overall X-ray spectrum is thermal; the breakout and tail are too faint to be measured individually.

ter modeled using more sophisticated magneto-hydrodynamic computer codes.

- Improve synchrotron spectra of PWNs and evaluate the break in the spectrum for specific objects to investigate the evolution of the energetic particle populations. This information can also help to better understand the process of particle injection by the pulsar.

- Measure expansions. Such measurements, of course, improve with longer time baselines.

A whole new era of being able to study the details of individual candidates in a significant sample of supernova remnants is upon us. The next generation of astronomers should have an exciting time solving many current problems.

Acknowledgments

My knowledge of the emission from SNRs has been gained from discussions with many colleagues of the years. I include here only those with whom I have worked on or specifically discussed Magellanic Cloud

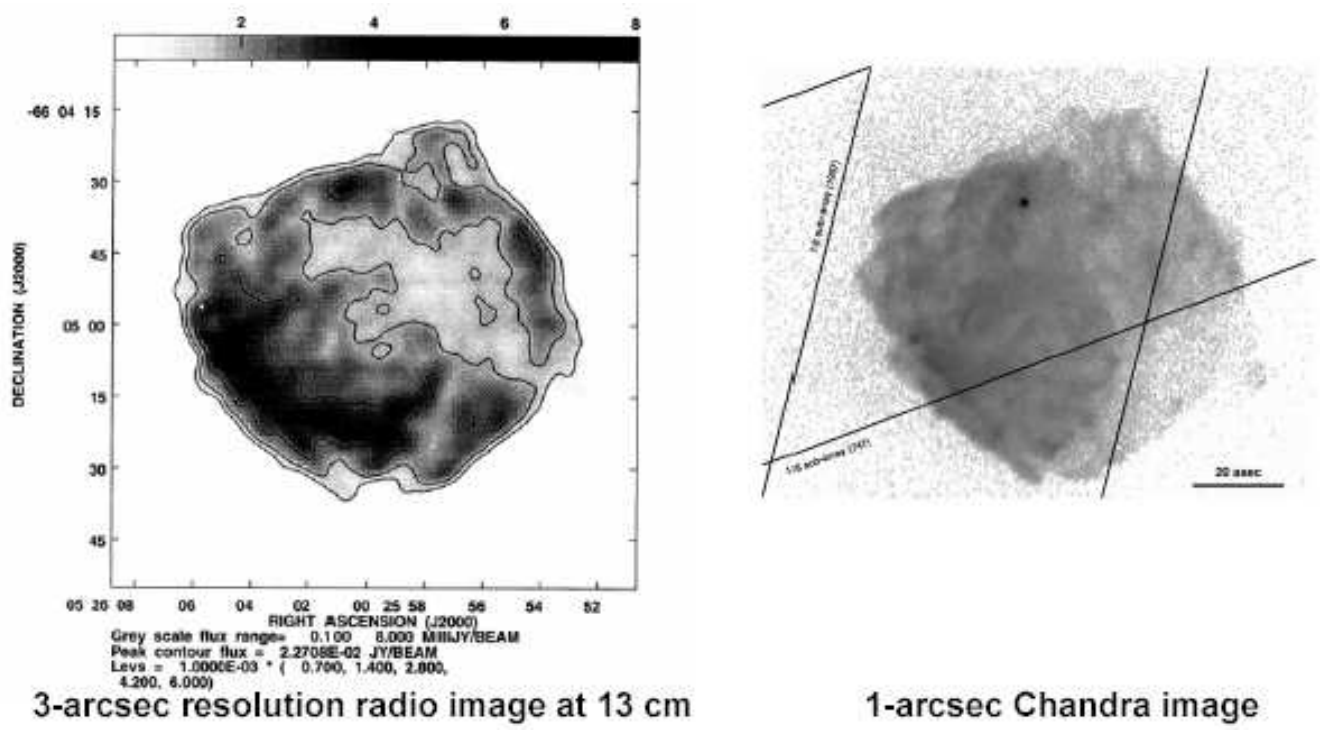

Figure 11: Radio and X-ray images of N49 showing the X-ray point source at the position of the SGR0525−66.

objects: S. Amy, L. Ball, M. Burton, L. Carter, R. Chevalier, Y.-H. Chu, H. Dickel, M. Filipovic, B. Gaensler, C. Gelino, E. Gotthelf, D. Green, R. Gruendl, P. Jones, N. Junkes, U. Klein, R. Klinger, J. Lazendic, V. McIntyre, D. Milne, R. Manchester, M. Mulligan, R. Petre, S. Reynolds, L. Staveley-Smith, F. Seward, P. Slane R. C. Smith, Q. D. Wang, P. F. Winkler, C. Wilkinson, R. Williams, and T. Ye. This research has been supported by an NSF Visiting Fellowship to the ATNF, NASA Grants NAG5-11159 and SAO GO3-4069B, and the Campus Honors Program of the University of Illinois at Urbana-Champaign.

References

Becker, R., Szymkowiak, A., Bolt, E., Holt, S., Serlemitsos, P. 1980, 240, L33

Chevalier, R. 1982, ApJ, 258, 790

Cox, D., Shelton, R., Maciejewski, W., Smith, R., Plewa, T., Pawl, A., Rózyczka, M. 1999, ApJ, 524, 179

Dickel, J., Chu, Y.-H., Gelino, C., Beyer, R., Burton, M., Milne, D., Spyromilio, J., Green, D., Wilkinson, C., Junkes, N. 1995, ApJ, 448, 623

Dickel, J., Milne, D. 1995, AJ, 109, 200

Dickel, J., Milne, D. 1998, AJ, 115, 105

Dickel, J.,Mulligan, M., Klinger, R., Gaensler, B., Milne, D., Manchester, R., Staveley-Smith, L., Kesteven, M., Gallant, Y. 2002, in Neutron Stars in Supernova Remnants, eds. P. Slane & B. Gaensler (ASP Conf. Series 271; San Francisco: ASP), 195

Gaetz, T., Butt, Y., Edgar, R., Eriksen, K., Plucinsky, P., Schlegl, E., Smith, R. 2000, ApJ, 534, L47

Gotthelf, E., Wang, Q. D. 2000 ApJ, 532, L117

Green, D. 2004, http://www.mrao.cam.ac.uk/surveys/snrs/

Hughes, J., Hayashi, I., Helfand, D., Hwang, U., Itoh, M., Kirshner, R., Koyama, K., Markert, T., Tsunemi, H., Woo, J. 1995, ApJ, 444, L81

Hughes, J., Smith, R. C. 1994, AJ, 107,1363

Kulkarni, S., Kaplan, D., Marshall, H., Frail, D., Murakami, T., Yonetoku, D. 2003, ApJ, 585, 948

Pannuti, T 2002, Duric, H., Lacey, C., Ferguson, K., Magnor, M., Mendelowitz, C. 2002, ApJ, 565, 966

Reynolds, S. 2005, in *"X-Ray and Radio Connections"*, eds. Sjouwerman, L. O. & Dyer, K. K., http://www.aoc.nrao.edu/events/xraydio

Rho, J., Petre, R. 1998, ApJ, 503, L167

Rothschild, R., Kulkarni, S., Lingenfelter, R. 1994, Nature, 368, 432

Sedov, L. 1959, Similarity and Dimensional Methods

in Mechanics, (New York: Academic Press)
Shelton, R., Cox, D., Maciejewski, W., Smith, R., Plewa, T., Pawl, A., Rózyczka, M. 1999, ApJ, 524, 192
White, R., Long, K. 1991, ApJ, 373, 543
Williams, R., Chu, Y.-H., Dickel, J., Gruendl, R., Seward, F., Guerrero, M., Hobbs, G. 2004, in preparation
Williams, R., Chu, Y.-H., Dickel, J., Smith, R. C., Milne, D., Winkler, P. F. 1999, ApJ, 514, 798
Ye, T., Amy, S., Wang, Q. D., Ball, L., Dickel, J. 1995, MNRAS, 275, 1218